urban science

MDPI

Article

A New and Easy Method to Determine the Energy Stored in Urban Areas: A Case Study of Mexico City

Martín Bonifacio-Bautista [1,2], Monica Ballinas [3] and Victor L. Barradas [2,*]

[1] Instituto de Ciencias de la Atmósfera y Cambio Climático, Universidad Nacional Autónoma de México, Ciudad de México 04510, Mexico; martin8722@live.com
[2] Instituto de Ecología, Universidad Nacional Autónoma de México, Ciudad de México 04510, Mexico
[3] Centro de Investigaciones en Ciencias de la Información Geoespacial, Ciudad de México 14240, Mexico; pd.mballinas@centrogeo.edu.mx
* Correspondence: vlbarradas@ecologia.unam.mx

Abstract: Urban areas present different climates from those of their rural surroundings. Energy balance and especially energy storage play important roles in the resulting climate since more than 50% of the net radiation is absorbed in densely urbanized areas. A simple model of energy storage in the urban fabric is presented, fed with the air temperature of a given area and its thermal properties; it can estimate heat storage (Q_S) with good results. The proposed Q_{ST} energy storage model was compared with Q_S results obtained from two sites in Mexico City, Escandón (objective hysteresis model, Q_{SOHM}) and ENP7 (residual, Q_{SRES}), and one site in Marseille, France (thermal mass scheme, Q_{STMS}). The comparison between Q_{ST} and Q_{SOHM} showed that $r^2 = 0.71$, while in ENP7 ($Q_N > 0$), Q_{SRES} and Q_{ST} were 116.5 Wm^{-2} and 142 Wm^{-2}, corresponding to 49% and 60% of the Q_N, respectively. The results obtained using the Q_{STMS} model in Marseille and Q_{ST} in Escandón showed similar behavior, with RMSEs of 109 and 101 Wm^{-2}, respectively, in a daily period. Although it is difficult to discern which method is better, it is possible to affirm that the presented method is quite accurate, easier to use, and inexpensive.

Keywords: urban energy balance; storage heat; urban heat island; urban heat

Citation: Bonifacio-Bautista, M.; Ballinas, M.; Barradas, V.L. A New and Easy Method to Determine the Energy Stored in Urban Areas: A Case Study of Mexico City. *Urban Sci.* **2024**, *8*, 244. https://doi.org/10.3390/urbansci8040244

Academic Editor: Luis Hernández-Callejo

Received: 20 September 2024
Revised: 26 November 2024
Accepted: 26 November 2024
Published: 4 December 2024

1. Introduction

Air movement and the boundary layer thermal structure are highly modulated by the planet's surface. Specifically, the energy balance—that is, the way energy is distributed and the resistance experienced by the surface—establishes vertical wind and surface and boundary layer temperatures. Urban areas change the material and aerodynamic makeup of the surface, greatly altering the superficial energy balance, along with the dynamic and thermodynamic nature of the boundary layer [1]. Cities generate their own climates due to the impact of urbanization; therefore, it is important to investigate the physical characteristics that produce this change through the energy balance to understand the resulting climate [2–5].

Urban development depends on the convergence of various factors, such as economic, demographic, cultural, political, social, geographical, and technological factors, as well as the way in which these interact with each other and the historical period in which they do so [6–8].

From the meteorology perspective, urban modifications manifest themselves in different ways: in mid-latitudes, solar radiation decreases, ambient temperature increases, relative humidity decreases, absolute humidity does not vary, total precipitation increases, and snow events decrease. The average annual wind speed decreases, and turbulence increases. The concentrations of gases, polluting particles, and condensation nuclei increase, and those of pollen decrease [9]. These alterations are not inevitably repeated in subtropical latitudes. In arid areas, due to anthropogenic actions, cities can behave like oases, with

lower air temperatures, higher humidities, and fewer polluting particles. Tropical cities surrounded by vegetation can experience changes like those of mid-latitude cities, with some variation caused by both latitudinal and socioeconomic differences, in addition to the greater formation of photochemical smog, lower annual thermal contrast, and less strict environmental legislation than those in extratropical countries [4,10,11].

Understanding how energy is transformed in cities is also necessary for engineers, architects, and/or city planners, who require detailed information on the airflow in urban areas to decide the structural strength and energy requirements of new constructions. This type of information is also necessary to feed numerical weather prediction models, making weather forecasting in urban areas a real possibility [12–14].

Although urbanization affects all elements of the energy balance, latent heat flux and energy storage (Q_S) present the most abrupt changes [15]. For densely urban areas, Q_S is of particular climatic importance since it has been shown that this component represents more than 50% of the net radiation in highly urbanized locations [11,16,17].

Energy storage depends on the materials and structure of the urban surface and its release at night, and it is considered an important contributor to the urban heat island effect [11,18]. Understanding this component is necessary in a variety of applications, not only for understanding the heat island but also, for example, to model sensible heat flux, evapotranspiration, and boundary layer growth. Therefore, it is necessary to determine the energy balance components, especially the Q_S. However, in many cases, this determination is difficult to carry out because it is necessary to use sophisticated and high-cost equipment, and the place where the determination is carried out is representative of a relatively small area compared to the urban area.

Heat storage is estimated mainly using three methods: (1) energy balance residual, (2) the objective hysteresis model (OHM) [19], and (3) the so-called mass scheme thermal insulation (TMS). The residual and OHM methods involve determining the energy balance, but they frequently overestimate the Q_S since there are components that are not considered and that do not allow for the closure of the energy balance, such as the heat generated by human activity. The TMS model requires the measurement of surface temperatures and temperatures at different depths of the materials of the buildings that make up the urban fabric, either with sensors such as thermocouples or with thermography, to understand the heat exchange between the built area and its surroundings. Cities contain varied materials, and their orientation makes this estimation almost impossible because the heating is uneven, so the estimation cannot adequately represent a certain area; therefore, the result is very imprecise. Furthermore, it is impossible to develop an analysis of significant errors for each method since they are open to one or more sources of errors that result from the instrumentation and/or method used.

This research introduces a simple and easy method to estimate Q_S within the urban fabric at different points in Mexico City. This method relies on meteorological variables, thermal properties, and urban morphological characteristics based on heating/cooling processes, which represent the behavior of urban materials throughout the day. It eliminates the need for sophisticated micrometeorological instrumentation and complicated estimation methods.

2. Materials and Methods

2.1. Study Site

Mexico City has a tropical climate modified by elevation. The average annual precipitation (=50 years) is 833 mm, of which 87% occurs in the wet season (June–November). The winds are light and mainly from the northeast. The maximum and minimum temperatures are recorded in April (28.6 °C) and January (4.9 °C), respectively [20], with a marked heat island effect in the urban area [21]. However, the urban heat island (UHI) effect is also established during the day, with intensities of up to 10 °C [17,22].

Table 1 presents the characteristics of the meteorological stations that were selected to carry out this research. These stations belong to the meteorological network of Mexico

City (RedMet), where air temperature and humidity, solar radiation, and the direction and intensity of the wind variables are systematically monitored. Most of the RedMet stations have operated since 1980. In contrast, the stations of Acolman (ACO) and Montecillo (MON) were also chosen to complement the thermal cooling/heating determinations as they present different land uses (Table 1 and Figure 1). In ENP7, the storage was determined as the residual of the energy balance. These measurements were made from December 1 to 14, 1998. All fluxes were measured, and the heat storage was calculated as residual [23].

Table 1. Location (latitude, Lat., °; longitude, Long, °; elevation, E, m asl) and population density (DP, inhabitants km^{-2}) of each of the meteorological stations (MSs) of the meteorological network of Mexico City used in this study.

MS	Lat	Long	E	DP
Acolman (ACO)	19°38′08″	98°54′43″	2198	1974
Escandón (ESC)	19°24′10″	99°24′10″	2165	8820
La Merced (MER)	19°25′29″	99°07′10″	2245	13,285
Esc. Nac. Preparatoria (ENP7)	19°25′08″	99°07′37″	2230	13,650
Montecillo (MON)	19°27′38″	98°54′10″	2252	642
Nezahualcóyotl (NEZ)	19°23′37″	99°01′42″	2235	16,900
Pedregal (PED)	19°12′31″	99°12′15″	2326	7894

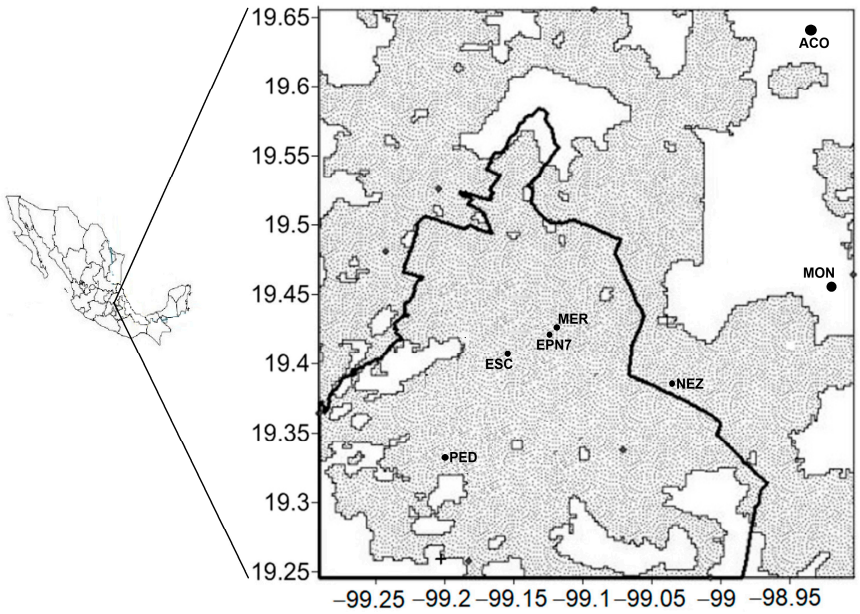

Figure 1. The study sites are located in Mexico City's metropolitan area. The shaded area represents the metropolitan area, and the solid line is the limit of Mexico City.

2.2. Heat Transfer Model

Estimates of Q_S at urban sites can also be derived from basic concepts of heat conduction and volumetric heat storage in a material, constructing a thermal mass scheme (TMS), in which measurements of surface temperature, thermal properties of materials, and construction are needed [24].

The proposed thermal model is based on the thermodynamic principle of heat storage calculation between its heat capacity and the heat transfer to store or release it. This model considers the response of the materials through the measurement of temperature since changes in ambient temperature carry information about the storage or release of said

heat. The model is given by the well-known relationship [24–26] derived from Newton's cooling law:

$$\Delta = \rho Cp\left(\frac{\Delta T_A}{\Delta t}\right)V \quad (1)$$

where ρ is the density of the material (kg m^{-3}), C_P is the specific heat of the material used (J kg^{-1} °C^{-1}), A is the area of the site (m^2), $\Delta T_A/\Delta t$ is the change in air temperature over time (°C h^{-1}), and V the volume (m^3) (Figure 2). That is, the energy that the material is capable of storing is measured based on the specific heat, the increase/decrease in air temperature, and the amount of material used. The model tells us that a change in temperature—in this case, of the air surrounding the urban fabric—causes a change in energy and that these changes provide a determination of the energy stored in the urban fabric, considering the thermal characteristics (ρCp) of the construction materials.

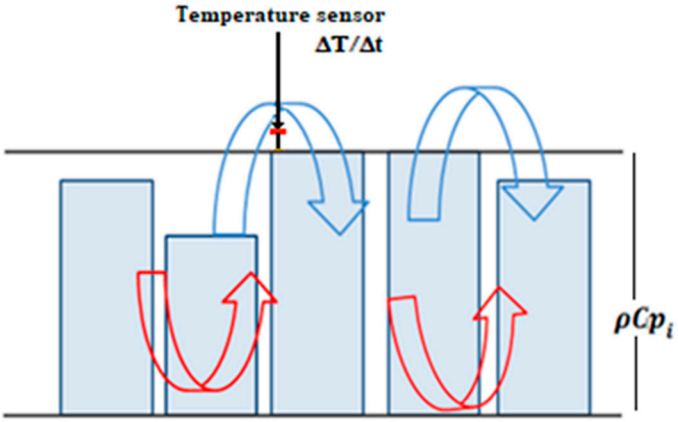

Figure 2. Convective heat transport in an urban module. The arrows represent turbulent flux going from an area of higher air temperature (red arrows) to areas of lower air temperature (blue arrows).

2.3. Thermal Slope

The thermal slope ($[\Delta T_A]/[\Delta t]$), or the increase/decrease in temperature, reflects not only the land use at the location where the thermometer is installed but also provides an in-depth view of how different land uses influence the air near the surface. This, in turn, determines changes in temperature and consequently helps estimate alterations in the components of the energy balance. The effect of land use on air temperature was estimated at the city sites. Thermal slopes were calculated from the minimum value to the maximum value (warming, from approximately 06:00 to 15:00 h) and from its maximum value to its minimum value (cooling, from approximately 03:00 to 06:00 h), expressed as the monthly average. Temperature data were taken at six sites within the metropolitan area to determine thermal slopes. Four of these sites included energy balance measurements, while the other two were selected to illustrate in greater detail the characteristics of these slopes based on land use.

2.4. Thermal Characteristics

Equation (1) was modified using a weighted average, which includes the various types of materials present in the urban area. These materials, which include solid and light blocks, metal structures (sometimes combined with vegetation), and glass, aluminum, or steel windows, are significant due to their high prevalence. Each type of material stores and releases heat in a different way, mainly due to its density and specific heat. Table 2 shows the density and specific heat values of materials used in urban construction.

Table 2. Density values (ρ, kg m^{-3}) and specific heat (C_P, J kg^{-1} °C^{-1}) of different construction materials [27].

Material	ρ	C_P
Solid lightweight concrete block	1000	1050
Solid brick	1800	1330
Light concrete	1000	1050
Light concrete block	1400	1050
Reinforced concrete	2400	1050
Adobe	1600	920
Gravel	1700	920
Topsoil	1800	920
Aluminum	2700	920
Glass	2500	840

The composition of buildings in the different study areas was determined (100 buildings in each site, chosen at random within a radius of 1 km), obtaining the percentages of the materials that constitute them. Of these, the most important structural compositions were concrete, concrete blocks, glass, and metal. Subsequently, these values were weighted based on the percentage of each of them in the structure, and the heat capacity that represented the buildings was obtained.

2.5. Urban Density

Urban density was estimated from dimensionless relationships proposed by [28], which determine how densely urbanized a given area is. Climatologically, the city's morphology is characterized in terms of the height, width, and density of its buildings. Grimmond and Oke [29] (1998) defined this morphometry of the study area (A_T) as surface dimensions, as follows:

$$\lambda_P = A_P A_T = L_X L_Y / D_X D_Y \quad \text{and } \lambda_F = A_F A_T = Z_H L_Y / D_X D_Y \tag{2}$$

where λ_F and λ_P refer to the densities of the frontal and plane constructions, respectively; A_P is the flat area of the element; A_F is the front (vertical) area of the element; L_X and L_Y are the length and width of the element, respectively; D_X and D_Y are the length and width of the total area (includes trees, streets, and some other elements), respectively; and Z_H is the height of the element. This characterization is not limited, so it could include houses of different shapes, winding streets, and dispersed trees that are typical of cities. These parameters were obtained using the Google Earth Pro program, with which the morphometry of the study sites was prepared.

For the purposes of urban density, only λ_P was used since it is what defines the density in a given area horizontally. To obtain λ_P for a given site, blocks were characterized based on sharing similar physical characteristics, mainly length and width. Four study sites were described: MER, ESC, PED, and NEZ, with a radius of 1 km around the micrometeorological station that comprise different forms of urban planning and land use. The characterization consisted of typical blocks within the study sites to obtain the main urban parameters.

2.6. Estimation of Q_{ST} at the Study Sites and Comparisons

Q_{ST} estimates were carried out at four sites in Mexico City: The Escandón, Nezahualcóyotl, Pedregal, and La Merced–Escuela Nacional Preparatoria 7 neighborhoods. These estimates were based on air temperature and the physical–thermal characteristics of the urban fabric. Subsequently, the Q_{ST} values were compared to the "real" values obtained from the energy balance measurements using the turbulent correlation method or the Eddy

correlation method [16,19,28]. In the Escandón district, Q_S was estimated in [30] using the objective hysteresis model (OHM) based on the proposal of Camufo and Bernardi [19] ($\Delta Q_{SOHM} = a_1 Q_N + a_2(dQ_N/dt) + a_3$, where Q_N is the net radiation, dQ_N/dt is the change in Q_N over time and a_1, a_2, and a_3 are the parameters of the model ($a_1 = 0.671$, $a_2 = 0.450$, and $a_3 = 52\ Wm^{-2}$). In this comparison, in the Escandón district, the Q_{SOHM} values were taken as the observed ones ("real," independent variable) and the Q_{ST} values as the "estimated" ones (dependent variable). To feed the models (Q_{SOHM} and Q_{ST}), measurements of net radiation and air temperature were carried out. Net radiation was measured using a net radiometer (NR-LITE2-L, Campbell Scientific) and air temperature using a hygrothermal probe (HMP155A-L, Campbell Scientific) at a height of 5 m from the roof of a 10 m high building. These instruments were connected to a data acquisition system (21XL, Campbell Scientific) performing scans every 20 s with averages stored every 30 min in the months of June and December 2021, the first month under unstable conditions (clear, cloudy skies), and in December under stable conditions (mostly clear skies).

In the ENP7 area, energy storage was estimated by determining the components of the energy balance using the parameterization and turbulent correlation techniques from the residual of the energy balance ($Q_{SRES} = Q_N - Q_E - Q_H$, where Q_E and Q_H are the latent and sensible heat fluxes, respectively). These measurements were carried out from December 1 to 14, 1998 [23]. However, and for this reason, it was necessary to include the area of La Merced, which is located less than 1 km from ENP7, to have air temperature data to feed the Q_{ST} model, thus giving the combination La Merced–Escuela Nacional Preparatoria 7 (MER-ENP7). As in Escandón, in this case, Q_{SRES} was taken as the independent variable and Q_{ST} as the dependent variable for comparison between the two methods. A third comparison was made with Q_S measurements carried out in Marseille, France, by Roberts et al. [24] using the TMS method (Q_{STMS}). These measurements in Marseille were carried out in the city center in a radius of 1 km, a site representative of the relatively homogeneous area. This site consists mainly of limestone buildings with an average height of 15.6 m, thick walls of 1 m, and sloping clay roofs. The measurements were made using a fixed infrared radiation thermometer network, infrared scanners, and thermistors from July 4 to 11, 2001, under stable synoptic conditions.

From the measurements in Marseille, the results of the thermal mass scheme (Q_{STMS}) were compared to the one presented (Q_{ST}) to observe the behavior of the proposed model, in addition to comparing the analysis obtained from the RMSE. From this comparison, the values obtained using the residual method and those predicted using the thermal mass scheme method were taken as the observed values. In the same way, the Escandón Q_{SOHM} values were taken as observed values, and the values resulting from the model were predicted. The period analyzed and compared focused on warm days, as they exhibited atmospheric stability and synoptic conditions similar to those in Marseille during the time of their measurements.

In Marseille, the average 3D surface coverage is 49% walls, 30% roofs, 13% impervious floor, and 8% vegetation [24]. Meanwhile, in the Escandón neighborhood, 58% is buildings, 37% is paving, and 5% is vegetation, which, according to the percentage of vegetation, indicates that they are both areas that share a high urban density.

3. Results and Discussion

Thermal slopes can represent a key factor in heat storage analysis since they reflect the heating/cooling of a surface. Different land uses, even if similar, modulate the temperature behavior differently, probably due to the urban density, vegetation density, and their spatial arrangement.

3.1. Thermal Slopes

Figure 3 shows the average hourly temperature in June and December in the selected sites. The analysis of the slopes shows that the different land uses, despite being similar, show different heating and/or cooling values. This is mainly due to the percentages of

the immersed materials and the ordering and orientation of each site. Table 3 shows these heating/cooling values, with PED in the winter season being the site that loses heat the slowest, while rural sites lose it the fastest. Likewise, the warming of rural sites is faster than that of urban sites. The slopes in June show the same behavior as that in the winter season (December); however, this analysis shows the rate at which the urban fabric cools or heats up, this being a first approximation of the heat capacity of these places.

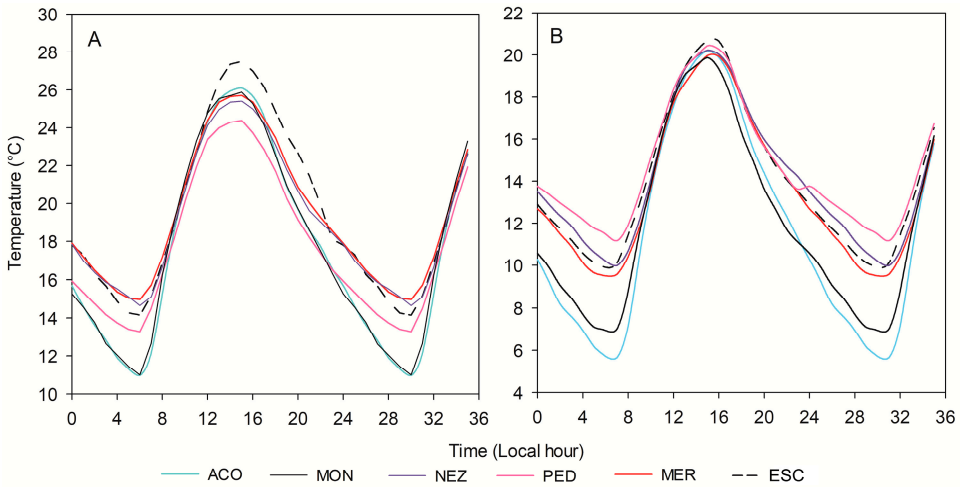

Figure 3. Average monthly hourly ambient temperature for the months of June (**A**) and December (**B**) in different sites in Mexico City (urban ESC, MER, PED, and NEZ) and two rural sites on the outskirts of the city (ACO and MON).

Table 3. Monthly average of the thermal slopes (°C h^{-1}) of the daily temperature progression in the months of June and December in different sites in Mexico City (urban HGM, MER, PED, and NEZ) and two rural sites on the outskirts of the city (ACO and MON).

Site	December		June	
	Heating	**Cooling**	**Heating**	**Cooling**
(ACO) Acolman	1.82	−0.91	1.78	−1.01
(ESC) Escandón	1.36	−0.68	1.48	−0.89
(MER) La Merced	1.34	−0.64	1.19	−0.71
(NEZ) Nezahualcóyotl	1.33	−0.64	1.19	−0.71
(PED) Pedregal	1.13	−0.56	1.23	−0.74
(MON) Montecillos	1.61	−0.81	1.78	−1.01

3.2. Urban Density

For the morphometry analysis, four sites were chosen (MER, ESC, PED, and NEZ) because heat flux measurements were carried out at these sites using the turbulent transfer method. This characterization consisted of establishing typical blocks or blocks within the study sites, with the purpose of obtaining the main urban parameters to determine the urban density (λp) since it is an important factor in setting the remaining morphological parameters and essential for the proposed thermal model in obtaining the Q_S component (Figure 4 and Table 4).

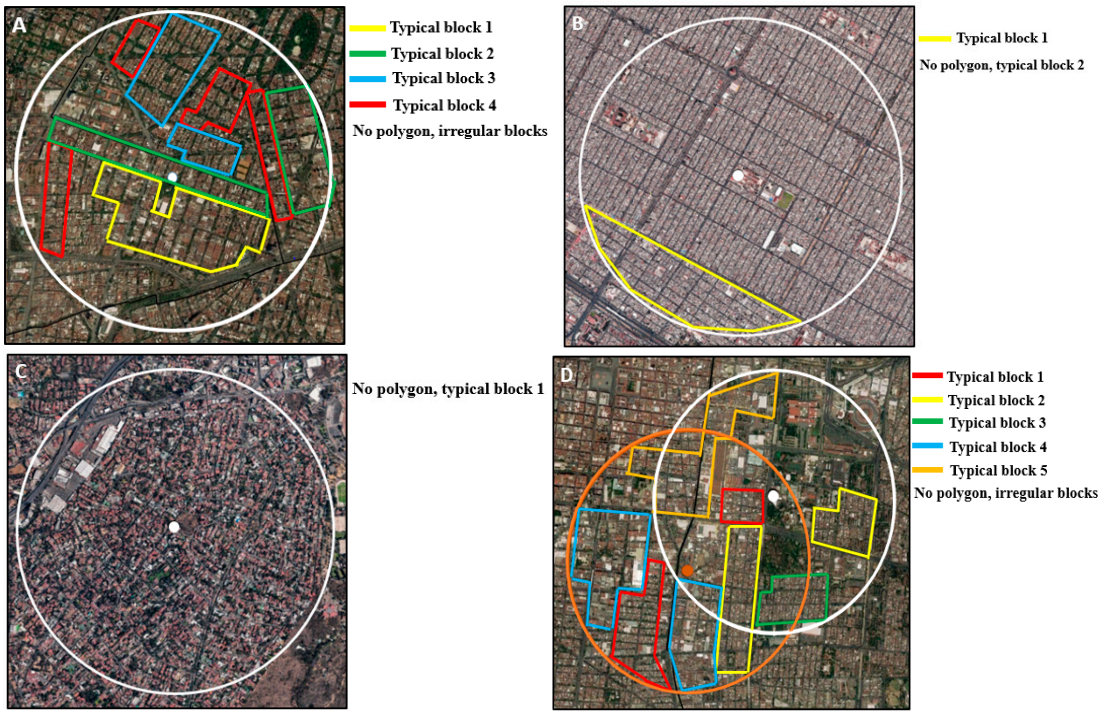

Figure 4. Characterization of blocks and land use in the districts of Escandón (**A**), Netzahualcóyotl (**B**), Pedregal (**C**), La Merced (**D**) (white point), and Escuela Nacional Preparatoria 7 (brown point) (Table 4).

Table 4. Morphometric characteristics of blocks from the Escandón (ESC), Nezahualcóyotl (NEZ), Pedregal (PED), and La Merced (MER) districts made up of typical blocks (TP), height (H, m), width (W, m), longitude (L, m), study area (A_T, m^2), the flat area of the element (A_P, m^2), and the front (vertical) area of the element (A_F, m^2). λ_F and λ_P refer to the densities of the flat and front constructions, respectively, with a total green area of 6.32 ha in Escandón, 3.14 ha in Nezahualcóyotl, 69.12 in Pedregal, and 49.2 in La Merced (Figure 4).

	H	W	L	A_T	A_P	A_F	λ_P	λ_F
ESC								
TP 1	14.4	84.8	225.3	414,320.3	343,618.9	21,912.7	0.83	0.05
TP 2	10.2	83.0	129.0	493,297.1	299,796.0	23,589.6	0.61	0.05
TP 3	8.5	39.8	158.5	319,797.3	170,110.1	13,314.8	0.53	0.04
TP 4	13.5	67.6	83.0	289,543.0	151,491.6	15,573.7	0.52	0.05
Irregular block	15.1	82.7	119.5	1,518,957.7	642,113.3	72,597.2	0.42	0.05
NEZ								
TP 1	7.6	35	226	2,801,600	1,580,960	21,912.7	0.56	0.02
TP 2	7.7	35	135	340,000	229,796	23,589.6	0.62	0.03
PED								
TP 1	5.6	22	29	3,141,600	662,666.5	21,912.7	0.21	0.04
MER								
TP 1	10.1	31	113.3	83,000	38,630.4	315.5	0.47	0.04
TP 2	8.5	43.3	166.7	288,860	216,666.7	368.3	0.75	0.04
TP 3	9.8	28	119.5	386,000	234,220.0	274.9	0.60	0.05
TP 4	9.4	97	170.3	230,000	99,085.5	910.3	0.43	0.02
TP 5	9.4	33	120.5	346,000	144,238.5	315.9	0.42	0.03
Irregular block	9.3	196	393.0	2,385,456	847,308.0	232.4	0.36	0.01

For the La Merced station, a λp of 0.5 was found with five typical blocks and one irregular; for Escandón, a λp of 0.58 was found with four typical blocks and one irregular; for Pedregal, a λp of 0.26 was found with a single configuration; for Nezahualcóyotl, a λp of 0.62 was found with two typical blocks. According to Grimmond and Oke [27], a λp that exceeds 0.5 is a densely urbanized area where buildings predominate. Escandón, La Merced, and Nezahualcóyotl are considered densely urban areas, but Pedregal is not a densely urbanized area. All of this is due to the distribution of buildings, parks, and vegetation in ridges.

The λp values obtained are comparable with sites such as Vancouver, Canada (suburban residential); Sacramento, CA (suburban residential); Arcadia, CA (suburban residential); Chicago, IL (suburban residential); Miami, FL (suburban residential); Los Angeles, CA (mixed residential); Los Angeles, CA (high-density single-family residential); Portland, OR (multifamily residential); Houston, TX (downtown core area)—with values of 0.62, 0.58, 0.53, 0.47, 0.35, 0.29, 0.27, 0.26, and 0.27, respectively [31–34]. The average construction height in La Merced–ENP7 was approximately 9 m, Escandón 12.5 m, Pedregal 6 m, and Nezahualcóyotl 7.6 m. These values are similar to sites such as San Francisco, CA; Boston, MA; Vancouver, BC; Albuquerque, NM; Austin, TX—with values of 9.7, 9.0, 6.8, 15.2, and 7.0 m, respectively [34,35] (Table 4).

3.3. Thermal Characteristics

In La Merced, vegetation occupies an area of 50.3 ha despite being a central site in the city. This is due to the green areas that surround it, such as La Plaza de la Soledad Park and Zapata Park. The built area spans 160.2 ha, with 103.7 ha of pavement, equivalent to 16%, 51%, and 33% of the area, respectively, without the presence of vacant lots or bodies of water. In contrast, the district of Nezahualcóyotl has the largest built area, where vegetation occupies only 1%, while the built area covers 61% and paving accounts for 37%, with no vacant lots or bodies of water (Table 5).

The values of the heat capacities were not used directly, because, for example, the heat capacity of concrete as the only material of the buildings would incur an error. Therefore, according to the analysis of the buildings, flat glass occupied 12%, metal approximately 2%, and concrete 86%, providing a weighted value of 1.203×10^6 J/m^{-3} °C^{-1} for the buildings.

Table 5. Land use in the different sites where energy balance measurements were carried out.

Site	Vegetation Cover/ Vacant Land (ha)	Built Coverage (ha)	Paved Coverage (ha)
La Merced	50.3	160.2	103.7
Nezahualcóyotl	3.14	191.6	116.2
Pedregal	66.0	128.8	119.4
Escandón	15.7	182.2	116.2

3.4. Thermal Model and Validation

3.4.1. Escandón Q_{ST} vs. Q_{SOHM}

The measurements made in the Escandón district in June show that Q_N reached values greater than 600 Wm^{-2}; however, there were days when Q_N was equal to or less than 300 Wm^{-2} due to the cloudiness produced by some meteorological phenomena. For $Q_N > 0$ in June, the average was 385 Wm^{-2} (Figure 5A). Meanwhile, in December, it reached values as high as 475 Wm^{-2}, with an average for $Q_N > 0$ of around 250 Wm^{-2} (Figure 5). The values obtained from Q_S using the OHM parameterized method show that when $Q_N > 0$, on average, it managed to store 50% with respect to Q_N on almost all the measured days. At the same time, Q_{ST} behaved very similarly to Q_{SOHM}, as can be seen in Figure 6 in both June (Figure 6A) and December (Figure 6B). The thermal model presents an acceptable general behavior since it follows the Q_{SOHM} pattern; however, the appropriate behavior

cannot be stated. It can also be seen that the thermal model presented greater variability than Q_{SOHM} during the morning.

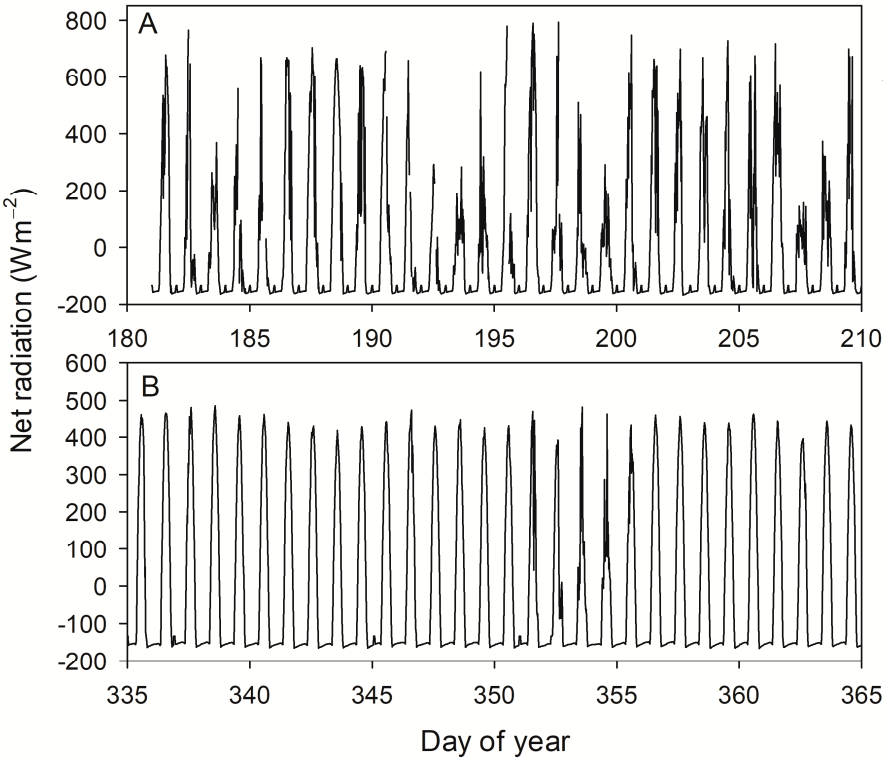

Figure 5. Net radiation measured in the Escandón neighborhood in June (**A**) and December (**B**) 2021.

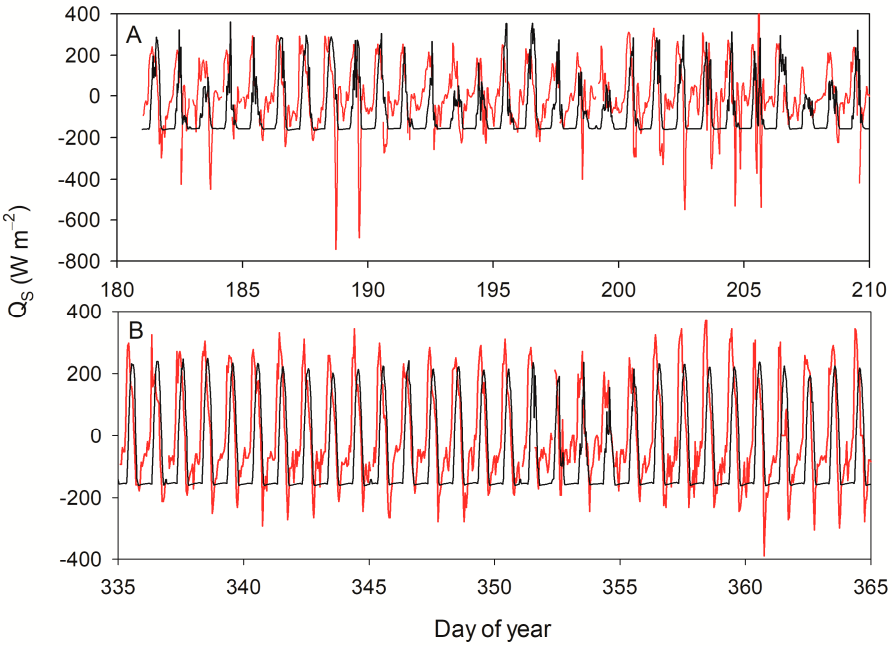

Figure 6. Comparison of the stored energy (Q_S) in the Escandón district obtained using the OHM (black line) and the thermal model (red line, Equation (1)) in June (**A**) and December (**B**) 2021.

The model showed significant variability, with minimum Q_{ST} peaks of up to -750 Wm^{-2} in June and 380 Wm^{-2} in December. This is probably due to the model's dependence on thermal slopes and the high thermal contrast that can occur from one day to the next. For example, the lowest peak in December was due to the passage of a cold front, causing the

thermal contrast to be much more marked until the temperature returned to a "normal" state after this event (Figure 6B). This leads us to determine that the thermal model is very sensitive to sudden changes in temperature and that the same will most likely happen in the presence of a heat wave, as shown by the negative peaks in June (Figure 6A).

There was also a lag in the stored energy over time calculated using the thermal model, which was determined to be 1.5 h (Table 6). This same correlation occurred on both warm (June) and cold days (December), so the data series was adjusted with a 1.5 h delay. Table 6 also shows that, although the best fit was 1.5 h, the time delay was more consistent on stable days, with a high coefficient of determination of 0.822 (December). In contrast, on warm days, the coefficient was lower (0.498, June). Additionally, it can be noted that the slope *a* value was almost 1 (0.996, a very close correspondence of 1:1) on stable days. However, as mentioned above, sudden changes in temperature affect the performance of the model. Nevertheless, despite this, the thermal model provides a very good estimate of energy storage in the urban fabric.

Table 6. Parameters of the simple regression analysis of the stored energy calculated or estimated using the proposed method (Q_{ST}) versus that estimated using the OHM method (Qs_{OHM}) ($Q_{ST} = aQ_{SOHM} + b$) for all data in June and December in the Escandón district in real time and delayed by 0.5, 1.0, 1.5, and 2.0 h. n = amount of data.

June				
a	***b* [Wm^{-2}]**	**r^2**	**hour**	**n**
0.376	32.70	0.112	0	1491
0.665	52.80	0.373	0.5	1480
0.760	58.05	0.494	1.0	1474
0.754	**57.06**	**0.498**	**1.5**	**1460**
0.698	52.77	0.416	2.0	1450
December				
0.569	29.69	0.269	0	1539
0.817	43.94	0.554	0.5	1520
0.965	52.64	0.771	1.0	1515
0.996	**54.29**	**0.822**	**1.5**	**1501**
0.923	49.93	0.708	2.0	1495

For the hourly averages of the measurement days, Q_{SOHM} and Q_{ST} showed very similar behavior, both on warm days and on cold days (Figure 6). The Q_{SOHM} model was 50% for Q_N when $Q_N > 0$ on warm days; the same behavior was maintained on cold days, at 52%. Q_S estimated with the thermal model was 42% of the Q_N for $Q_N > 0$ in June, while in December, it was 34%. The difference between June under stable atmospheric conditions was 8%, while in December, it was 18% (greater stability). It is not known for sure which of the two methods is the most accurate, but it is evident that the thermal model has fewer errors.

Based on the Q_{ST} values in the Escandón district, the storage behavior was similar to that obtained in Sacramento, CA; Marseille, France; Miami, FL; Basel, Switzerland; Los Angeles, CA; Vancouver, BC—at 0.26, 0.28, 0.30, 0.36, 0.40, and 0.48, respectively, for residential land use [9,36,37].

3.4.2. La Merced–ENP7 Q_{ST} vs. Q_{SRES}

The estimation of Q_{ST} with respect to the values obtained from residual Q_S in ENP7 (Q_{SRES}) showed that the behaviors are very similar, although the thermal model at night continued to show a drop in values (Figure 7), according to the results obtained from the

energy flux at the ENP7 site [24]. The average $Q_N > 0$ at this site was 237 Wm^{-2}, while Q_{SRES} was 116.5 Wm^{-2}, which corresponds to 49% of the Q_N, and the Q_{ST} estimate was 142 Wm^{-2}, which is equivalent to 60% of the Q_N. In a simple regression of Q_{ST} vs. Q_{SRES}, it was found that $Q_{ST} = 1.059Q_{SRES} + 9.768$ ($r^2 = 0.877$, $p < 0.001$, slope very close to 1, thus indicating a good relationship between Q_{ST} and Q_{SRES} with a systematic error of 9.678 Wm^{-2}). The results of the thermal model for this land use, Q_{ST}/Q_N, show that it is a densely urban area since its values are comparable with other sites where measurements have been made in similar atmospheric conditions and at a similar time of year: Cosmo, Japan; Beijing, China; Tokyo, Japan—at 0.63, 0.66, and 0.62, respectively [38,39].

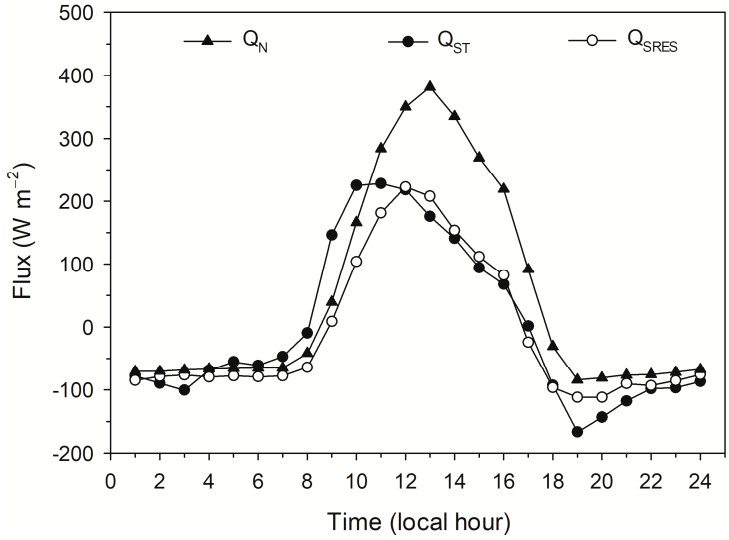

Figure 7. Comparison of the stored heat fluxes estimated with the thermal model (Q_{ST}) and the residual energy balance (Q_{SRES}) at the La Merced–ENP7 National Preparatory School.

3.4.3. Q_{ST} vs. Marseille Q_{SRES} and Q_{STMS}

Figure 8 shows the Q_{ST} values of the Escandón district and the Q_{STMS} and Q_{SRES} in Marseille, France. The behavior of the three models was similar; however, at night/early morning, Q_{STMS} presented higher values, while in the afternoon/night, it presented lower values for Q_{SRES} when $Q_N > 0$, with an average of 345 Wm^{-2}, and Q_{SRES} and Q_{STMS} were 21% and 15%, respectively, of Q_N. This difference in percentages (6%) should be zero, as already described previously in the Q_{ST} results for the Escandón district. Figure 9 shows the behavior of Q_{SRES}, Q_{STMS}, and Q_{ST} with similar variations detected in the statistical analyses despite not corresponding to the same region.

In this case, the RMSE analysis compared the predicted values with those observed in both the Escandón and Marseille areas, where several temperature measurement instruments were used to obtain the energy storage values with greater precision through the thermal mass scheme. The comparison with the proposed method involved a greater number of instruments. The daily root mean square deviation (RMSE) of Marseille was 109 Wm^{-2}, while that obtained in Escandón using the thermal model was 101 Wm^{-2}. For daytime hours ($Q_N > 0$) in Marseille, the RMSE was 137 Wm^{-2}, and in the Escandón district, it was 133 Wm^{-2}; for nighttime hours ($Q_N < 0$) in Marseille, a value of 62 Wm^{-2} was obtained, while in Escandón, it was 71 Wm^{-2}.

In several investigations, the hysteresis method (OHM) of Camufo and Bernardi [20] was used, which accounts for residual Q_S as observed values in the RMSE analysis. The daily RMSE values for places such as Sacramento, CA (residential suburb), Chicago, IL (residential suburb), Marseille (downtown), and Tucson, AZ (residential suburb), were 66, 83.3, 95, and 107.4 Wm^{-2}, respectively. The RMSE value of the daily Q_{ST} is similar to these values, as shown in previous studies [23,24,37,40].

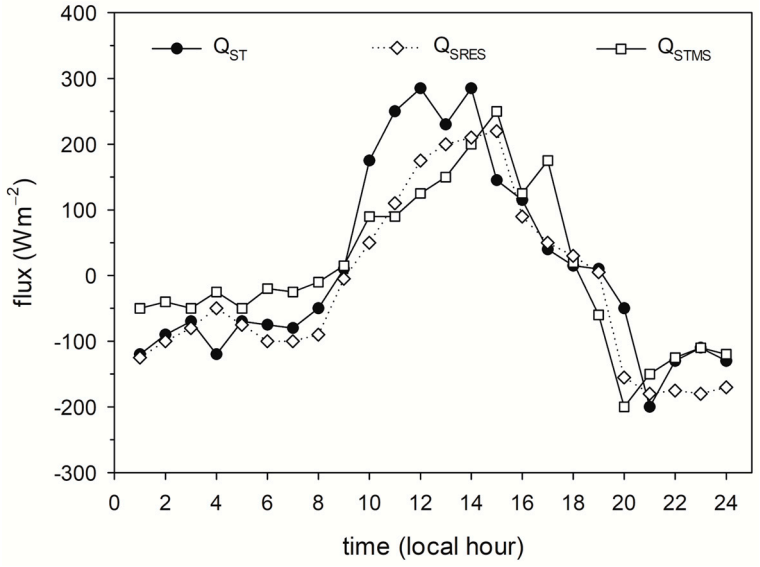

Figure 8. Energy storage measured in Marseille, France, showing the energy storage derived from the energy balance residual (Q_{SRES}) and that obtained using the thermal mass scheme model (Q_{STMS}) and the proposed thermal model (Q_{ST}) in the Escandón district.

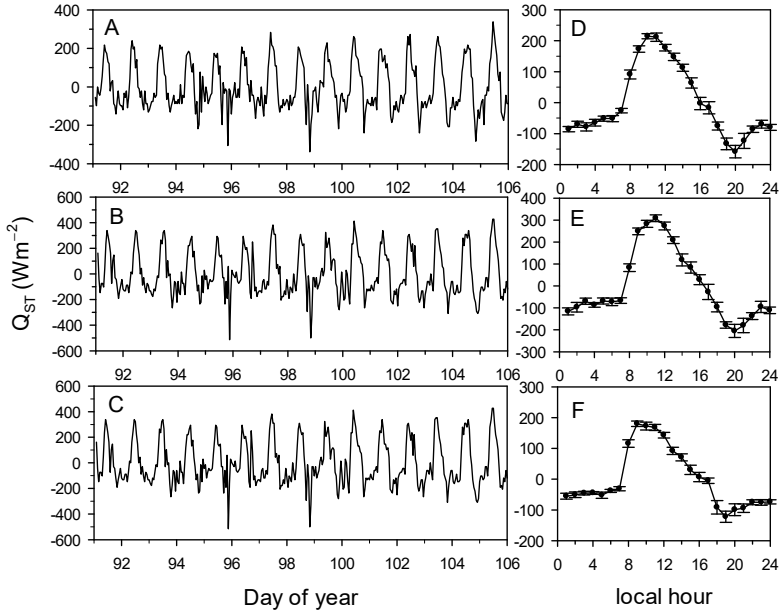

Figure 9. Stored energy estimates using the thermal model (Q_{ST}) in April (**A**–**C**) and average (**D**–**F**) of La Merced (**A**,**D**), Nezahualcóyotl (**B**,**E**), and Pedregal (**C**,**F**).

A comparison of this study with observations from 403 cities in Asia, Europe, and the United States showed that the characteristics of the urban surface energy balance are mainly affected by climatic conditions, followed by surface properties. Basel, Switzerland, and Marseille, France, have Mediterranean climates with hot, dry summers and warm, rainy winters. The latter is reflected in the case of MER–ENP7, since its analysis was carried out in the winter period, in which Q_S reached 60% of the Q_N and, for example, Cosmo and Tokyo in Japan, where the July–August period had a Q_S/Q_N ratio of 0.53 and 0.26, respectively, while in the December–February period, the same sites reached 0.63 and 0.62, increasing the value of Q_S.

3.4.4. Estimation of Q_S in Other Parts of the City Using the Thermal Model

The thermal model is applicable to any point where ambient temperature measurements are made, and the type and percentage of materials used in urbanization can be determined. The Q_{ST} results from April 1 to 15, 2019, can be seen in Figure 9. As the energy balance measurements made in Mexico were performed close to this time of year, Q_{ST} was estimated for this period. The values in MER, NEZ, and PED were 116, 157, and 95 Wm^{-2}, respectively. According to the bulletins of the National Meteorological Service on April 5 and 6, 2019, a frontal system occurred in the border region of northeastern Mexico, which interacted with an area of instability in the north of the country and affected the states from the center of the country, including Mexico City. These days coincide with the first fall in the peak Q_{ST} values. Meanwhile, on April 9, a cold front generated the potential for very strong storms in Mexico City. The meteorological phenomena that affected the country were recorded in the results, which proves that the model is very sensitive to sudden changes in temperature.

3.4.5. Generalities

Unfortunately, the proposed model cannot be compared with data from other cities, such as Tokyo in Japan, because there is no continuity in the measurement campaigns or because research is only limited to specific cases, such as the wet or hot season. One of the purposes of this study was to facilitate the acquisition of a key component of the energy balance in urban sites, which can be applied in fields such as meteorological studies, urban planning, and architectural planning.

The analysis of different methods in Marseille proves what has been said, which is useful and encouraging since it cannot be considered a standard method or technique. These approximations of the different methods are completely dissimilar, including measurement, modeling, and parameterization. They also vary in the simplicity of application; the broad convergence of their results is, therefore, very satisfactory. The OHM [19], which uses averaged values of net radiation and simple surface properties to estimate Q_S, does not perform as well at the Marseille site as at several other urban sites [24]. Although it provides rational estimates overall, the model does not capture the short-term temporal characteristics or the degree of hysteresis between Q_S and Q_N.

As is known, the residual method provides a good approximation; however, it carries all the errors of the measurements. The Marseille TMS model is based on surface and air temperature gradients with considerable variations between different features of an urban system as a result of differences in surface materials, orientation, and wind flow. Ambient temperatures incorporating a wide variety of surface facets can provide more stable results. However, the proposed model needs improvement, as sudden changes in temperature destabilize it over this period.

4. Conclusions

The thermal model is easy to apply and functional, providing clear estimates of energy storage in the urban fabric. It is also inexpensive, requiring only one thermometer to track temperature changes over time. However, it appears to have two sources of error: one due to the approximations in the morphometric–thermal determination of the study sites and another due to sudden changes in temperature caused by various synoptic and local phenomena capable of changing the temperature suddenly by more than 3 °C. Comparisons made with real energy storage values showed that the model is reasonably accurate, but further verification is needed with additional results and across other sites. Additionally, the model would benefit from the inclusion of a parameter to account for the delay in the values it presents, probably caused by heat-dissipative media. It is recommended that this model be applied on days with atmospheric stability. Despite these limitations, it remains difficult to determine which model best expresses reality, as the hysteresis model (OHM), the thermal mass scheme (TMS), and the residual model all introduce errors in other components of the energy balance.

Author Contributions: M.B.-B.: conceptualization, data curation, investigation, methodology, and writing. V.L.B.: conceptualization, investigation, methodology, project administration, supervision, visualization, writing, and reviewing and editing. M.B.: conceptualization, data curation, investigation, validation, and writing. All authors have read and agreed to the published version of the manuscript.

Funding: This research was granted by the Programa de Apoyo a Proyectos de Investigación e Innovación Tecnológica, DGAPA, UNAM (grant IT200620), and CONACyT-México (grant no., 550297).

Data Availability Statement: Data will be made available upon request.

Acknowledgments: This research was granted by the Programa de Apoyo a Proyectos de Investigación e Innovación Tecnológica, DGAPA, UNAM (grant IT200620). The first author thanks the Postgraduate in Earth Sciences of the Universidad Nacional Autónoma de México, CONACyT-México (grant no., 550297) for the scholarship awarded.

Conflicts of Interest: The authors declare that they have no known competing financial interests or personal relationships that could have appeared to influence the work reported in this paper.

References

1. Harman. The Energy Balance of Urban Areas. Ph.D. Thesis, The University of Reading, Reading, UK, 2003.
2. Barradas, V.L. Evidencia del efecto de "Isla Térmica" en Jalapa, Veracruz, México. *Geofísica* **1987**, *26*, 125–135.
3. Barradas, V.L.; Tejeda-Martínez, A.; Jáuregui, E. Energy balance measurements in a suburban vegetated area in Mexico City. *Atmos. Environ.* **1999**, *22*, 4109–4113. [CrossRef]
4. Oke, T.R.; Zeuner, G.; Jauregui, E. The surface energy balance in Mexico City. *Atmos. Environ.* **1992**, *26B*, 433–444. [CrossRef]
5. Grimmond, C.S.B.; Blacket, M.; Best, M.; Barlow, J.F.; Baik, J.; Belcher, S.E.; Steeneveld, G.J. The International Urban Energy Balance Models Comparison Project: First Results from Phase 1. *J. Appl. Meteorol. Climatol.* **2010**, *49*, 1268–1292. [CrossRef]
6. Centeno, J.C. Población y medio ambiente. *Interciencia* **2002**, *27*, 217.
7. Alcañis, M. Cambios demográficos en la sociedad global. *Papeles Población* **2008**, *57*, 227–254.
8. Carreño, C.C.; William, H.A. Relación entre los procesos de urbanización, el comercio internacional y su incidencia en la sostenibilidad urbana. *Cuad. Vivienda Urban.* **2018**, *11*, 1–10. [CrossRef]
9. Tejeda, A. Sobre mediciones y parametrizaciones del balance energético y la estabilidad atmosférica en la Ciudad de México. Ph.D. Thesis, The Universidad Nacional Autónoma de México, México City, Mexico, 1996.
10. Grimmond, C.S.B.; Oke, T.R. Comparison of heat fluxes from summertime observations in the suburbs of four North American cities. *J. Appl. Meteorol.* **1995**, *34*, 873–889. [CrossRef]
11. Oke, T.R.; Spronken-Smith, R.A.; Jáuregui, E.; Grimmond, C.S.B. The energy balance of central Mexico City during the dry season. *Atmos. Environ.* **1999**, *22*, 3919–3930. [CrossRef]
12. Bornstein, R.D.; Thompson, W.T. Effects of frictionally retarded sea breeze and synoptic frontal passages on sulfur dioxide concentrations in New York City. *J. Appl. Meteorol.* **1981**, *20*, 843–858. [CrossRef]
13. Bornstein, R.; Lin, Q. Urban heat islands and summertime convective thunderstorms in Atlanta: Three case studies. *Atmos. Environ.* **2000**, *34*, 507–516. [CrossRef]
14. Rozoff, C.M.; Cotton, W.R.; Adegoke, J.O. Simulation of St. Louis, Missouri, land use impacts on thunderstorms. *J. Appl. Meteorol.* **2003**, *42*, 716–738. [CrossRef]
15. Cervantes-Pérez, J.; Vargas-Sánchez, M.A.; Barradas, V.L. Clima, urbanización y uso del suelo en ciudades tropicales de México. *Ciudades* **2002**, *51*, 19–24.
16. Ching, J.K.S. Urban-scale variations of turbulence parameters and fluxes. *Bound.-Layer Meteor.* **1985**, *33*, 335–361. [CrossRef]
17. Ballinas, M.; Barradas, V.L. The urban tree as a tool to mitigate the urban heat island in Mexico City: A simple phenomenological model. *J. Environ. Qual.* **2016**, *45*, 157–166. [CrossRef]
18. Barradas, V.L. La isla de calor urbana y la vegetación arbórea. In *Oikos*, 7th ed.; Instituto de Ecología UNAM: Coyoacán, Mexico, 2013; pp. 16–19.
19. Camufo, D.; Bernardi, A. An observational study of heat fluxes and their relationships with net radiation. *Bound. Layer Meteorol.* **1982**, *23*, 359–368. [CrossRef]
20. SMN. Servicio Meteorológico Nacional. Available online: https://smn.conagua.gob.mx/es/climatologia/informacion-climatologica/normales-climatologicas-por-estado?estado=df (accessed on 20 July 2023).
21. Jauregui, E. Heat island development in Mexico City. *Atmos. Environ.* **1997**, *31*, 3821–3831. [CrossRef]
22. Ballinas, M. Mitigación de la isla de calor urbana a partir de la vegetación arbórea. Master's Thesis, Universidad Nacional Autónoma de México, Mexico City, Mexico, 2011.
23. Tejeda, M.A.; Jáuregui, E. Surface energy balance measurements in the México City region: A review. *Atmósfera* **2004**, *18*, 1–23.
24. Roberts, S.M.; Oke, T.R.; Grimmond, C.S.B.; Voogt, J.A. Comparison of four methods to estimate urban heat storage. *J. Appl. Meteorol.* **2006**, *5*, 1766–1781. [CrossRef]
25. Brazo, R.M. Sistema Pasivo de Almacenamiento de Energía Térmica en Centrales Termosolares. Bachelor's Thesis, Universidad de Sevilla, Sevilla, Spain, 2016.

26. Grande, R.A. Estado del Arte de Sistemas de Almacenamiento de Energía Térmica Mediante Cambio de Fase, a Media y Alta Temperatura. Bachelor's Thesis, Universidad de Sevilla, Sevilla, Spain, 2016.
27. *Real Decreto 2429/1979*; Por el que se Aprueba la Norma Básica de Edificación NBE-CT-79, Sobre Condiciones Térmicas en los Edificios. Agencia Estatal del Boletín Oficial del Estado: Madrid, Spain, 1979; Volume 53, pp. 24524–24550.
28. Oke, T.R. *Boundary Layer Climates*, 2nd ed.; Routledge Taylor & Francis Press: Abingdon, UK, 1987; p. 435.
29. Grimmond, C.S.B.; Oke, T.R. Aerodynamic properties of urban areas derived from analysis of surface Form. *J. Appl. Meteorol.* **1998**, *38*, 1262–1291. [CrossRef]
30. Velasco, E.; Pressley, S.; Grivicke, R.; Allwine, E.; Molina, L.T.; Lamb, B. Energy balance in urban Mexico City: Observations and parameterization the MILAGRO/MCMA-2006 field campaign. *Theor. Appl. Climatol.* **2011**, *103*, 501–517. [CrossRef]
31. Voogt, J.; Oke, T. Complete urban surface temperatures. *J. Appl. Meteorol.* **1997**, *36*, 1117–1132. [CrossRef]
32. Burian, S.J.; Brown, M.J.; Linger, S.P. *Morphological Analyses Using 3D Building Databases: Los Angeles, California*; LA-UR-02-0781; Los Alamos National Laboratory: Los Alamos, NM, USA, 2002.
33. Burian, S.J.; Velugubantla, S.P.; Chittineni, K.; Maddula, S.; Brown, M.J. *Morphological Analyses Using 3D Building Databases: Portland, Oregon*; LA-UR-02-6725; Los Alamos National Laboratory: Los Alamos, NM, USA, 2002.
34. Burian, S.J.; Han, W.S.; Brown, M.J. *Morphological Analyses Using 3D Building Databases: Houston, Texas*; LA-UR-; Los Alamos National Laboratory: Los Alamos, NM, USA, 2003.
35. Schläpfer, M.; Lee, J.; Bettencourt, M.A. Urban Skylines: Building heights and shapes as measures of city size. *Phys. Soc.* **2015**, arXiv:1512.00946.
36. Cleugh, H.A.; Oke, T.R. Suburban-rural energy balance comparisons in summer for Vancouver, B.C. *Bound-Layer Meteorol.* **1986**, *36*, 351–369. [CrossRef]
37. Grimmond, C.S.B.; Oke, T.R. Heat storage in urban areas: Local-scale observations and evaluation of a simple model. *J. Appl. Meteorol.* **1999**, *38*, 922–940. [CrossRef]
38. Miao, S.; Dou, J.; Chen, F.; Li, J.; Li, A. Analysis of observations on the urban surface energy balance in Beijing. *Sci. China Earth Sci.* **2012**, *55*, 1881–1890. [CrossRef]
39. Hu, D.; Yang, L.; Zhou, J.; Deng, L. Estimation of urban energy heat flux and anthropogenic heat discharge using aster image and meteorological data: Case study in Beijing metropolitan area. *J. Appl. Remote Sens.* **2012**, *6*, 63559–63618. [CrossRef]
40. Lemonsu, A.; Grimmond, C.S.B.; Masson, V. Modeling the surface energy balance of the core of an old Mediterranean City: Marseille. *J. Appl. Meteorol.* **2004**, *43*, 312–327. [CrossRef]